Interactions Among Emissions, Atmospheric Chemistry, and Climate Change: Implications for Future Trends

Chien Wang and Ronald G. Prinn

Abstract

To gauge the overall effect of complex interactions among emissions, atmospheric chemistry, and climate, we have conducted a series of simulations on 120-year time scales, using a global coupled chemistry-climate model along with various predictions of anthropogenic emissions and different assumptions for chemistry and climate model parameters. To specifically identify the impacts of chemical species on climate change, we have also carried out sensitivity runs which include or exclude radiative effects due to increasing concentrations of greenhouse gases, and sulfate aerosols produced from anthropogenic sulfur emissions.

Interactions among emissions, atmospheric chemistry, and climate are known to be complex. Based on current predictions of increasing future anthropogenic emissions, the climate will likely warm by some uncertain amount in the next century. The cooling effect caused by sulfate aerosols can offset a certain amount of this warming (about 20%, in our tests), but not the whole amount.

It has been found that emissions of CH_4, CO, NO_x, and SO_2 significantly influence the tropospheric concentrations of several important chemical species. Specifically, our simulations indicate that the average tropospheric OH concentration in the year 2100 will be 16–31% lower than its current level. As a result of this reduction, the predicted lifetimes of certain chemical species increase as we move into the next century. For example, in the year 2100 the lifetimes of CO and CH_4 increase by 2 months and 2.5 years respectively from their current estimates. Also, we find that the overall influence of climatic variations on chemistry is less than that due to the increasing trends of emissions, especially for CH_4.

Climatic variations can still subtly impact many chemical patterns in the troposphere through changes in water vapor, temperature, rainfall, and cloud-cover patterns. However, predicted changes in climate do not reverse the overall trends of changing chemistry represented by the reduction in tropospheric OH concentration and related increases in the lifetimes of chemical species, which are driven primarily by the increasing emissions.

1. Introduction

Long-term trends of chemical species in the atmosphere are determined by emissions from anthropogenic and natural sources as well as by atmospheric transport, physical and chemical processes, and deposition. While continually increasing emissions of such trace species as CO_2, N_2O, and CH_4 are predicted to raise global temperatures *via* the "greenhouse effect" (IPCC, 1996), growing emissions of SO_2 (which form sulfate aerosol through oxidation) most likely will have a cooling effect by reflecting solar radiation back to space. Complicating matters is the fact that atmospheric chemical reactions themselves are sensitive to climate change, being functions of temperature, solar ultraviolet fluxes, and water vapor content. Natural emissions of some chemical species can also change significantly as a result of climatic variations (Liu, 1996; Prinn *et al.*, 1997). Such intricate feedbacks—chemical processes and natural emissions themselves being affected by climate changes they have influenced—obfuscate understanding of the overall effects of the complex interactions involving emissions, chemical reactions, biological processes, and climate change.

Submitted to the *Journal of Geophysical Research* (September 1997)

Climate impact of increasing atmospheric concentrations of long-lived gaseous species and short-lived aerosols have become one of the most widely discussed issues in atmospheric science, as summarized in IPCC (1994, 1996). We know that the current tropospheric chemical composition is quite different from the one in the pre-industrial era as a result of changed emissions of CH_4, CO, NO_x, and SO_2 (*e.g*., Crutzen and Zimmermann, 1991; Thompson, 1992; Derwent, 1996; Levy II *et al*., 1997). However, prediction of future long-term (≥ 100 years) changes of both atmospheric composition and climate requires considering interactions among emissions, chemistry, and climate and is a major challenge at the present time.

To elucidate these complex interactions, we have conducted a series of simulations on a 120-year time scale, using a global coupled chemistry-climate model (Wang *et al*., 1997; Sokolov and Stone, 1997) along with predictions of anthropogenic emissions provided by a global economic development model (Yang *et al*., 1996). Given emission predictions or specifications, our model calculates long-term trends in zonally-averaged distributions of radiatively and chemically important species, as well as all the important climate variables. To identify the impacts of chemical species on climate change, on the one hand, and of climate change on chemical processes, on the other, we have also carried out sensitivity runs which include or exclude radiative effects due to increasing concentrations of greenhouse gases, and sulfate aerosols produced from anthropogenic sulfur emissions.

Details of the model, along with a comparison of modeled results and observations, predicted spatial distributions and temporal evolution of chemical species, and predictions of key climate parameters, are described in a companion paper (Wang *et al*., 1997). Concentrations of chemical species in the atmosphere from 1977 to 1995, as predicted using this model, agree reasonably well with observed data obtained from the global monitoring networks (*e.g*., Cunnold *et al*., 1994; Novelli *et a.l*, 1992). This paper provides analyses and discussion focusing primarily on the interactions in this model among emissions, chemistry, and climate. A description of the model and the design of several numerical experiments are presented first, followed by discussion of the computed relative effects on climate of radiatively important species and sulfate aerosols, based on results from sensitivity runs. Features of the interactions among emissions, chemical processes, and climate as revealed in this study are then presented, followed by some conclusions.

2. Design of Numerical Experiments

Our model is two-dimensional (zonal-averaged), with fully coupled treatments of chemistry and climate. It has 24 latitude bands and nine pressure levels (Wang *et al*., 1997; Sokolov and Stone, 1997; Prinn *et al*., 1997). This model computes the evolution of 25 chemical species that are radiatively or chemically important in the atmosphere, such as CO_2, chlorofluorocarbons, CH_4, N_2O, CO, NO_x, O_3, HO_x, SO_2, and sulfate aerosols, as well as the evolution of climate variables and other physical parameters. In order to simulate chemical distributions, the chemistry sub-model takes into account 41 gas-phase and 12 heterogeneous reactions, along with emissions, dry and wet deposition, and transport by winds and convection. The radiative forcing by climate-relevant gases and sulfate aerosols is calculated in the climate sub-model using the predicted chemical concentrations. Calculations of transport, chemical reaction rates, and deposition fluxes of chemical species are made in turn by using meteorological variables calculated by the climate sub-

model. The system is fully coupled with the two sub-models communicating with one another with 20 minute, hourly, and five hourly, time steps for transport, physics, and radiation, respectively. For the runs described in this study the model was integrated over a period of 124 years (1977 to 2100).

Emissions of CO_2, CH_4, N_2O, $CFCl_3$, CF_2Cl_2, CO, NO, and SO_2 are included. Except for chlorofluorocarbons, all chemical emissions have both *natural* and *anthropogenic* components; both components are functions of latitude, and include many sub-components. The present simulation treats total annual natural emissions as constant over time: the annual natural emissions of CH_4, N_2O, CO, NO (excluding lightning), and sulfur are: 130 Tg, 9.1 Tg(N), 158.6 Tg(C), 10 Tg(N), and 12.8 Tg(S), respectively, while production of NO by lightning is specified as 5 Tg(N). Values for anthropogenic emissions in this study are based on predictions of the MIT Emission Prediction and Policy Analysis (EPPA) Model (Yang *et al.*, 1996).

To illustrate a range of plausible predictions, we carried out a series of numerical experiments in each of which one of three plausible assumptions were made regarding the following processes: (1) emissions due to human activity, (2) aerosol radiative forcing intensity and speed of oceanic uptake of CO_2 and heat, and (3) sensitivity of the climate sub-model to doubling CO_2. The three assumptions are identified using the labels: H for the "high" case, R for the "reference" case, and L for the "low" case—all labels being determined by the effect of the plausible assumption on the surface temperature predicted in the year 2100. Each run is then designated by listing the labels for the three processes in the order given above. For example, the "HHH" run consists of high anthropogenic emissions, low aerosol radiative forcing intensity with slow oceanic uptake of CO_2 and heat, and high sensitivity of the climate sub-model to doubled CO_2—a combination leading to the highest temperature change in the year 2100.

To focus our discussion on interactive features, we carried out nine experiments, using three different emission predictions (the first of the three labels) in combination with three selected combinations of chemistry-climate settings (the second and third labels). To investigate the influence of sulfate aerosols and other radiatively important species on climate, we also carried out two additional experiments using the "reference" emissions and chemistry-climate settings, except that one test was conducted without the anthropogenic sulfate aerosol radiative forcing predicted by the chemistry sub-model (designated RRR-NA), while the other was conducted using the monthly-mean concentrations of greenhouse gases and aerosols predicted during 1990 for calculations of radiative forcing in all years beyond 1990 (designated RRR-NF).

Values for the high, reference, and low integrated emissions in the three emission predictions are displayed in Table 1; specific assumptions for the total of 11 experiments conducted are displayed in Table 2.

Table 1. Integrated emissions between 1977 and 2100 for chemicals in high (H), reference (R), and low (L) emission predictions.

	$CFCl_3$ (Tg)	CF_2Cl_2 (Tg)	N_2O (PgN)	NO_x (PgN)	CO_2 (PgC)	CO (PgC)	CH_4 (Pg)	SO_2 (PgS)
H	5.27	7.52	1.98	8.55	1912.28	98.27	110.89	13.94
R	5.27	7.52	1.94	8.40	1654.83	97.05	105.73	13.39
L	5.27	7.52	1.91	8.26	1368.73	95.73	100.21	12.86

Table 2. Designs of numerical experiments.

	Emissions	Aerosol Forcing/Ocean Uptake[1]	Climate Sub-model Sensitivity[2]
HHH	high	low/slow	high
HRR	high	reference/reference	reference
HLL	high	high/fast	low
RHH	reference	low/slow	high
RRR	reference	reference/reference	reference
RLL	reference	high/fast	low
LHH	low	low/slow	high
LRR	low	reference/reference	reference
LLL	low	high/fast	low
RRR-NA	reference	none[3]/reference	reference
RRR-NF	reference	fixed[4]/reference	reference

[1]Calculated optical depths of anthropogenic sulfate aerosols including direct and indirect effects are multiplied by 2 for the high and 0.5 for the low aerosol forcing setting; ocean vertical diffusion coefficients for heat and CO_2 are five times larger or smaller than their reference value for fast or slow ocean uptake, respectively.

[2]Climate sub-model sensitivity is defined as difference in global average surface temperature between doubled CO_2 and current-day equilibrium climates. The value is 3.5, 2.5, and 2.0 ^oC for the high, reference, and low setting respectively.

[3]No aerosol forcing (the chemistry sub-model still calculates evolution of SO_2 and sulfate).

[4]All calculations of radiative forcings due to major greenhouse gases and sulfate aerosols after 1990 use the predicted mean monthly concentrations of these substances during 1990.

3. Trends in and Climatic Effects of Chemistry

As a result of increasing emissions, our model predicts that concentrations of long-lived species such as CO_2, CH_4, and N_2O will increase significantly through the year 2100. In the "reference" (RRR) run, the global mean mole fraction in 2100 is predicted to be 745 ppm (parts per million) for CO_2, 410 ppb (parts per billion) for N_2O, and 4.4 ppm for CH_4. Due to these increased concentrations of major greenhouse gases, the global mean surface temperature climbs by 2.5 ^oC from its 1990 value by the end of the 21st Century.

In the RRR-NF sensitivity run, the radiative forcing by long-lived gases and sulfate aerosols beyond 1990 were calculated using monthly average concentrations predicted by the model during 1990 rather than predictions for those future years as in RRR. All other parameters, including those involved in atmospheric chemistry, remained identical to those used in the reference run (RRR). Comparing the latitudinal distributions of monthly mean surface temperatures predicted by the RRR-NF run to those predicted by the RRR run (Figure 1), we find that the combined climate effects of all chemical species lead to a warming trend that appears much more significant at high latitudes, due to changes in oceanic and atmospheric heat transport and surface properties such as ice and snow cover in these high latitude areas. In contrast to the more than 3.5 ^oC increase in the surface temperature at high latitudes, noticeable warming does not appear in tropical areas until the year 2050, and a moderate 1.5 to 2.0 ^oC increase occurs only during the last 10 years of the 21st Century.

A comparison of surface temperatures obtained from the reference run with those obtained from another sensitivity run, RRR-NA, in which anthropogenic sulfate aerosol forcing is neglected, shows that the cooling effect of sulfate aerosol is also more significant at high latitudes of the Northern Hemisphere than in tropical regions (Figure 2), although more detailed analysis indicates that most radiative forcing due to sulfate aerosols exists around 40 ^{o}N. At high latitudes in the Northern Hemisphere ($\geq$ 60 ^{o}N), the cooling effect of sulfate aerosols is 1 to 1.5 ^{o}C currently, and according to the model, may increase to more than 2.5 ^{o}C later in the 21st Century.

Increasing CH_4 and CO emissions also significantly change tropospheric chemistry. All our simulations show that OH concentrations in the year 2100 are reduced 16 to 31% from current levels, the greatest decline occurring between the years 2000 and 2040. As a result of this reduction, the chemical lifetimes of CH_4, CO, and SO_2 will lengthen beyond current estimates as we move into the next century. For example, the lifetime of CO lengthens from 3 months currently to about 5 months in the year 2100, and the lifetime of CH_4 would be more than 11.5 years by then, compared to the current estimate of 9 years. We note that our modeled current-day lifetimes of these species closely approximate recent estimates for them based on OH levels determined from CH_3CCl_3 observations (Prinn *et al.*, 1995).

Although our model indicates the concentrations of OH will change significantly, its spatial and temporal patterns are expected to remain similar to the current ones in the year 2100. These patterns are influenced primarily by latitudinal and seasonal changes. For example, the highest values for the CH_4 destruction rate by OH shift from the Southern Hemisphere during winter to the Northern Hemisphere during summer (Figure 3). The reaction CH_4 + OH primarily occurs close to the subtropical surface, due to the temperatures and higher densities there, and to the temperature-dependence of its rate constant.

Conducting the same sort of analysis for CO destruction yields a different result, as shown in Figure 4. The center of photochemical destruction of CO moves less significantly with season, and also expands into the middle and high troposphere relative to CH_4, due to its temperature-independent rate constant and concentrated emissions in the Northern Hemisphere.

A distribution similar to that for CO destruction occurs for sulfate photochemical production (Figure 5), although its production rates differ more markedly among the various seasons. The highest production rates appear in the Northern Hemisphere midlatitudes in summer, close to the Earth's surface. Despite changes in their absolute values, all these processes—the photochemical destruction of CH_4 and CO, and production of sulfates—show very similar distributions to their current ones in the year 2100 according to the model predictions.

4. Influence of Emissions and Climate on Chemistry

An important application of our model is in the study of feedback mechanisms among emissions, chemistry, and climate. Here we present the influence of emissions and climate variations on chemical processes, especially in the troposphere, by comparing results of eleven sensitivity runs.

The different emission scenarios, aerosol forcing, oceanic uptake, and climate sensitivity in these runs produce markedly different results in terms of climate change predictions. For example, projected increases in surface temperature from the current level to the year 2100 range from

1.34 ºC for the LLL run to 5.06 ºC for the HHH run; associated changes in global-average water vapor concentration for these same scenarios during the same time period range from 6.7% to 33.4%. The different temperature projections in turn accelerate or retard the chemical reaction rates, and also important, the different water vapor concentration projections affect significantly the concentration of OH radicals in the troposphere, and thus the chemical lifetimes of many species. Emissions, especially CO_2, CH_4 and CO, play significant roles in generating all these changes.

Table 3 displays the lifetimes of the chemical species CO, CH_4, SO_2, and NO_x, as defined by their gas-phase chemical losses in the various runs, based on the average, over the entire integration period (124 years), of their monthly mean values. Also listed are relative changes (in percent) of surface temperature and tropospheric mean water vapor concentrations from 1977 to 2100. The first three groups (denoted A, B, and C) of runs each shows results from three runs with the same chemistry-climate model assumptions but different emission scenarios. The average lifetimes for CO, CH_4, and SO_2, derived from all the high-emission runs, are respectively about 6%, 4%, and 2% longer than the lifetimes derived from all the low-emission runs. This result

Table 3. Average lifetimes during the period from 1977 to 2100 of several photochemically active species and under various specified conditions and groupings.

Group	Run[1]	CO (months)	CH_4 (years)	SO_2 (days)	NO_x (days)	$(\Delta T/T_{1977}) \times 100$ (%)[2]	$(\Delta Q/Q_{1977}) \times 100$ (%)[3]
A	HLL	4.44	11.07	17.42	1.139	12.2	6.7
	RLL	4.32	10.87	17.27	1.141	10.5	6.7
	LLL	4.17	10.63	17.07	1.144	10.0	6.7
B	HRR	4.34	10.78	16.88	1.138	20.0	14.9
	RRR	4.23	10.61	16.79	1.141	19.2	15.3
	LRR	4.09	10.39	16.63	1.142	16.2	12.0
C	HHH	4.16	10.29	15.96	1.136	37.4	33.4
	RHH	4.06	10.16	15.94	1.138	31.3	27.4
	LHH	3.95	10.00	15.87	1.140	27.5	23.6
D	LHH	3.95	10.00	15.87	1.140	27.5	23.6
	LRR	4.09	10.39	16.63	1.142	16.2	12.0
	LLL	4.17	10.63	17.07	1.144	10.0	6.7
E	RHH	4.06	10.16	15.94	1.138	31.3	27.4
	RRR	4.23	10.61	16.79	1.141	19.2	15.3
	RLL	4.32	10.87	17.27	1.141	10.5	6.7
F	HHH	4.16	10.29	15.96	1.136	37.4	33.4
	HRR	4.34	10.78	16.88	1.138	20.0	14.9
	HLL	4.44	11.07	17.42	1.139	12.2	7.6
G	RRR	4.23	10.61	16.79	1.141	19.2	15.3
	RRR-NF	4.30	10.84	17.24	1.141	0.7	0.8

[1]See Tables 1 and 2 for explanations of the nomenclature of the various runs.

[2]$\Delta T = T_{2100} - T_{1977}$, T_{2100} and T_{1977} represent annual-mean and global-average surface temperatures in the years of 2100 and 1977 respectively.

[3]$\Delta Q = Q_{2100} - Q_{1977}$, Q_{2100} and Q_{1977} represent annual-mean and tropospheric-average water vapor mixing ratios in the years of 2100 and 1977 respectively.

occurs regardless of the fact that all else equal the high-emission cases provided warmer temperatures and higher water vapor concentrations than the low-emission runs. This suggests that higher emissions, although generating more OH (due to higher water vapor concentrations associated with the warmer temperatures), result in lower concentrations of OH overall, which is caused by the increased destruction of OH induced by the higher emissions and hence higher concentrations of CO and CH_4. In contrast to the above three species, the average lifetime of NO_x appears to change less significantly. The NO_x lifetime is slightly shorter in the high-emission cases than in the low-emission cases, in part because gas-phase chemical destruction of NO_x is inversely proportional to temperature.

Rearranging these results by listing together runs with the same emissions (yielding groups D, E, and F in Table 3), we find differences to be somewhat more between the low and the high chemistry-climate parameter cases than between the low and high emission cases in groups A, B, or C. Note also that the differences in temperature and water vapor change are much more significant within groups D, E, and F. The warmer cases, when compared to the cooler cases for any given emission, result in shorter lifetimes for all species listed in Table 3, apparently due to higher water vapor concentrations and consequently more OH in the troposphere. Interestingly, within each group, relationships between temperature change and chemical lifetimes in groups D, E, and F are opposite to those found for groups A, B, and C, except in the case of NO_x. The relationships among emissions, chemistry, and climate are apparently very complicated, and—most important—under certain circumstances the influence of emissions can offset the influence of climate variations, and *vice versa*.

These complications are also revealed by Figure 6, in which the lifetimes of CO (Figure 6a), CH_4 (Figure 6b), SO_2 (Figure 6c), and NO_x (Figure 6d) in group E runs (reference emissions with different chemistry-climate settings) are plotted as functions of annual-mean surface temperature. The CO, CH_4, and SO_2 in the cooler run (RLL) have overall longer lifetimes than in the two other runs shown (RRR and RHH) due to the relatively lower H_2O and hence OH concentrations in RLL. In contrast, in each individual run, lifetimes of these species increase with temperature (and time) primarily because increasing emissions with time reduce OH concentrations. This indicates that, by itself, the long-term decline in tropospheric OH concentration that occurs due to growing CH_4 and CO emissions in all these runs is actually more important to the evolution of tropospheric chemistry than are the relative changes produced by varying the emission scenarios or climate-chemistry model parameters.

One interesting question is: how different from our reference run would these atmospheric chemical properties be if we assume the current climate will continue through the end of the next century, regardless of any emission-induced change in atmospheric chemical composition? Comparing results in Table 3 (group G) from Run RRR-NF with those from Run RRR, we find that the average lifetimes of CO, CH_4, and SO_2 in Run RRR-NF are respectively about 1.7%, 2.2%, and 2.7% longer than those in the case of Run RRR, although the average lifetime of NO_x remains about the same. This shows that even without a change in climate, increasing emissions—especially of CH_4 and CO—can still significantly change atmospheric chemical properties. From Figure 7, we can see that the OH concentration is even lower in the case of Run RRR-NF than in the case of Run RRR (7.7×10^5 *vs*. 8.2×10^5 radicals/cm^3 in the year 2100) due to a lack of compensation in RRR-NF from increased water vapor concentration. Consequently, the lifetimes

of CO and CH_4 in Run RRR-NF lengthen compared to those in Run RRR, leading to higher concentrations of these compounds in the atmosphere. The tropospheric mean mole fractions of CO and CH_4 in Run RRR-NF are respectively about 10 ppb and 200 ppb higher than those in Run RRR.

Sulfur emissions are, of course, an important factor in determining sulfate aerosol concentrations in the troposphere. We found that the global maximum optical depth of sulfate aerosol each year increases nearly linearly with annual sulfur emissions (Figure 8). Because global sulfur emissions are concentrated in a rather small, midlatitude northern hemispheric band, the global maximum conversion of anthropogenically emitted sulfur to sulfate is proportional to sulfur emission in that region. The concentration of sulfate aerosol in any specific area and the overall properties of sulfate aerosols in the troposphere are also significantly influenced by climate parameters.

Figure 9 shows the correlation between the surface optical depth of sulfate aerosols and surface temperature at each latitude, taking into consideration accompanying precipitation rates. The correlations are derived using monthly-mean data from our 124-year integration (1488 months in total), in the reference Run RRR. It appears that, beyond a threshold temperature, the optical depths of sulfate aerosols increase exponentially with temperature in warmer regions with low precipitation rates (< 3.0 mm/day, represented in Figure 9 by red dots). This is mainly due to higher OH concentrations at higher temperatures, although the envelope of the red curves in the figure indicate some difference between cooler high latitudes (left-hand curves) and warmer low latitudes (right-hand curves). On the other hand, in regions with heavy precipitation (≥ 3.0 mm/day, represented by blue dots), the dependence of the sulfate aerosol optical depth on temperature almost disappears below 25 ^{o}C. Our model runs show that wet scavenging is a very important factor in determining sulfate aerosol concentrations, and hence their climatic effects. Neglecting consideration of the wet scavenging of sulfate aerosol, our model would produce quite a different radiative forcing, especially in specific regions.

5. Discussion and Conclusions

Interactions among emissions, atmospheric chemistry, and climate are known to be very complicated. Both emissions and climate variations can effectively influence the evolution of chemical species in the atmosphere by altering their rates of chemical reaction and affecting their surface fluxes. Of particular importance are climatic and emission processes modifying the concentrations of key free radicals such as OH. On the other hand, changing concentrations of chemical species can in turn influence climate, through aerosol-related cooling and greenhouse gas-related warming. To understand better such issues, we developed a coupled two-dimensional (zonally-averaged) model including both a climate sub-model and a chemistry sub-model. A number of sensitivity runs, differing from one another in their assumptions about major uncertain parameters governing emissions and climate, have provided significant insights into key interactions among chemistry and climate.

Based on our assumed estimates for increasing future anthropogenic emissions, we have found that the climate warms in the next century but by very uncertain amounts. The cooling effect caused

by sulfate aerosols offsets a certain amount of warming (about 0.5 ^{o}C, in our runs), but not the whole effect.

It has been found in this study and in some others (*e.g.*, Crutzen and Zimmermann, 1991; Thompson, 1992; Derwent, 1996) that emissions of CH_4 and CO, as well as other chemical species such as NO_x and SO_2, significantly influence the tropospheric concentrations of several important chemical species, including OH, SO_2, NO_x, CH_4, and CO. Specifically, in our study the simulations indicated that the average tropospheric OH concentration in the year 2100 will be 16 to 31% lower than its current level. As a result of this reduction, the lifetimes of CH_4, CO, and SO_2, lengthen significantly beyond their current values as we move into the next century. For example, the lifetime of CO in the year 2100 is predicted to become two months longer than currently, while the lifetime of CH_4 that same year would exceed its current value by 2.5 years. Also, we found the overall influence of emissions on chemistry to exceed the influence of climate when significantly increasing emissions, especially of CH_4, are maintained.

Climate variations can, however, still subtly impact many chemical properties of the troposphere. Higher water-vapor concentrations associated with warming, for example, help offset a certain amount of the emission-induced reduction in OH concentration. However, no predicted changes in climate overwhelm the predicted changing chemistry represented by the reduction in tropospheric OH concentration and related increases in the lifetimes of chemical species. Sustenance of OH at current levels in the future would require the trends of increasing emissions to be halted or reversed.

The present study, when considered along with previous work, raises serious questions concerning possible future changes in the chemical composition of the troposphere lowering the capacity of atmospheric reactions to process ever increasing emissions. Research on this issue is becoming increasingly significant to the understanding of climate.

Acknowledgments

We thank our MIT colleagues Andrei Sokolov, Peter Stone, Xiangming Xiao, Yuexin Liu, and Gary Holian for significant help and advice and for access to their models and model results. Jean Fitzmaurice provided help with emission calculation. Zili Yang, Henry Jacoby and their colleagues provided EPPA model outputs for anthropogenic emissions. Judy Stitt assisted in editing the manuscript.

References

Crutzen, P.J., and P.H. Zimmermann, The changing photochemistry of the troposphere, *Tellus*, 43AB, 136–151, 1991.

Cunnold, D.M., P.J. Fraser, R.F. Weiss, R.G. Prinn, P.G. Simmonds, B.R. Miller, F.N. Alyea and A.J. Crawford, Global trends and annual releases of CCl_3F and CCl_2F_2 estimated from ALE/GAGE and other measurements from July 1978 to June 1991, *J. Geophys. Res*., 99, 1107–1126, 1994.

Derwent, R.G., The influence of human activities on the distribution of hydroxyl radicals in the troposphere, *Phil. Trans. R. Soc. Lond.* A, 354, 501-531.

IPCC, *Climate Change 1994: Radiative Forcing of Climate Change and an Evaluation of the IPCC IS92 Emission Scenarios*, Cambridge Univ. Press, Cambridge, UK, 339 p., 1994.

IPCC, *Climate Change 1995*: *The Science of Climate Change*, Cambridge Univ. Press, Cambridge, UK, 572 p., 1996.

Liu, Y., 1996, Modeling the emissions of nitrous dioxide (N_2O) and methane (CH_4) from the terrestrial biosphere to the atmosphere, MIT Joint Program on the Science and Policy of Global Change Report No. 10, Cambridge, MA, 219 p., 1996.

Novelli, P.C., L.P. Steele and P.P. Tans, Mixing ratio of carbon monoxide in the troposphere, *J. Geophys. Res*., 97(D18), 20,731–20,750, 1992.

Prinn, R.G., R.F. Weiss, B.R. Miller, J. Huang, F.N. Alyea, D.M. Cunnold, P.J. Fraser, D.E. Hartley and P.G. Simmonds, Atmospheric trends and lifetime of CH_3CCl_3 and global OH concentrations, *Science*, 269, 187-192, 1995.

Prinn, R.G., H. Jacoby, A. Sokolov, C. Wang, X. Xiao, Z. Yang, R. Eckaus, P. Stone, D. Ellerman, J. Melillo, J. Fitzmaurice, D. Kicklighter, G. Holian, and Y. Liu, Integrated global system model for climate policy assessment: Feedbacks and sensitivity studies, submitted to *Climatic Change*, 1997.

Sokolov, A.P., and P.H. Stone, A flexible climate model for use in integrated assessments, MIT Joint Program on the Science and Policy of Global Change, Report No. 17, Cambridge, MA, 16 p., submitted to *Climatic Change*, 1997.

Thompson, A.M., The oxidizing capacity of the Earth's atmosphere: Probable past and future changes, *Science*, 256, 1157-1165, 1992.

Yang, Z., R.S. Eckaus, A.D. Ellerman and H.D. Jacoby, The MIT Emissions Prediction and Policy Analysis (EPPA) Model, MIT Joint Program on the Science and Policy of Global Change Report No. 6, Cambridge, MA, 49 p., 1996.

Wang, C., R.G. Prinn, and A. Sokolov, A global interactive chemistry and climate model, MIT Joint Program on the Science and Policy of Global Change Report No. 24, Cambridge, MA, 49 p., submitted to *J. Geophys. Res*., 1997.

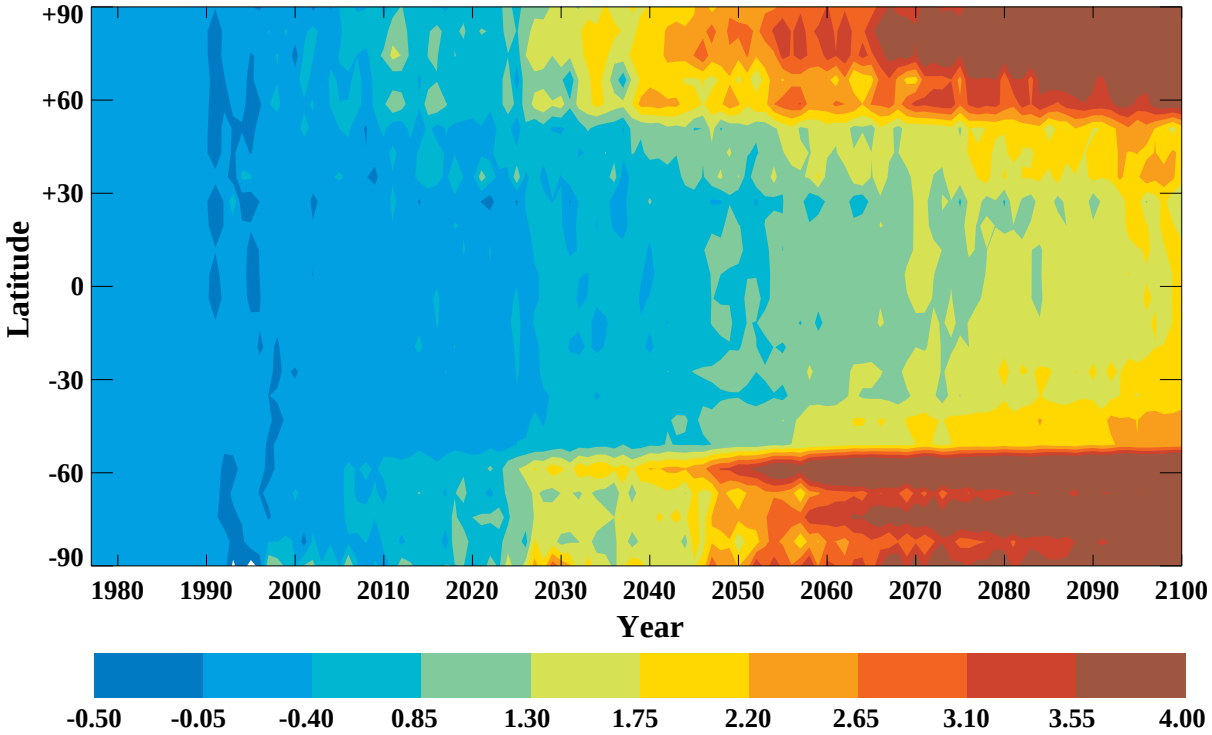

Figure 1. Differences between model predicted monthly-mean surface temperatures (T_g) derived from the reference run (RRR) and those from the sensitivity run RRR-NF, expressed as functions of latitude and time in ^oC.

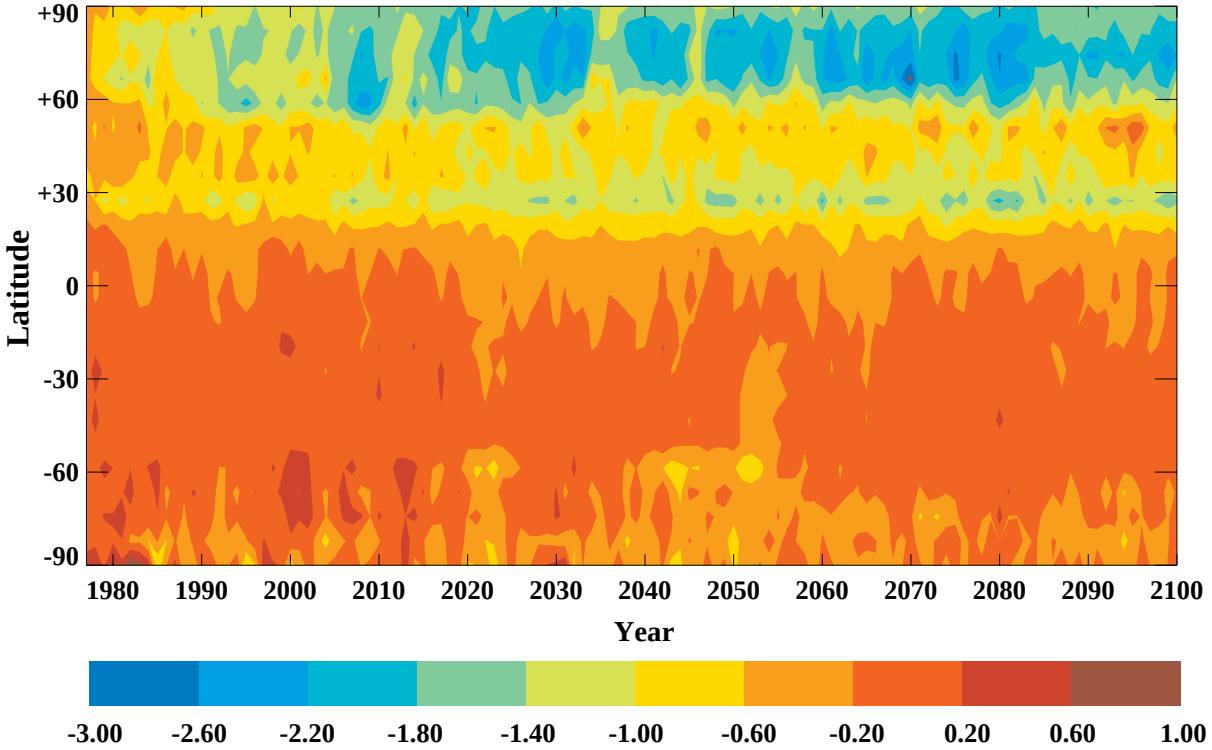

Figure 2. Differences between model predicted monthly-mean surface temperatures (T_g) derived from the reference run (RRR) and those from the sensitivity run RRR-NA, expressed as functions of latitude and time in ^oC.

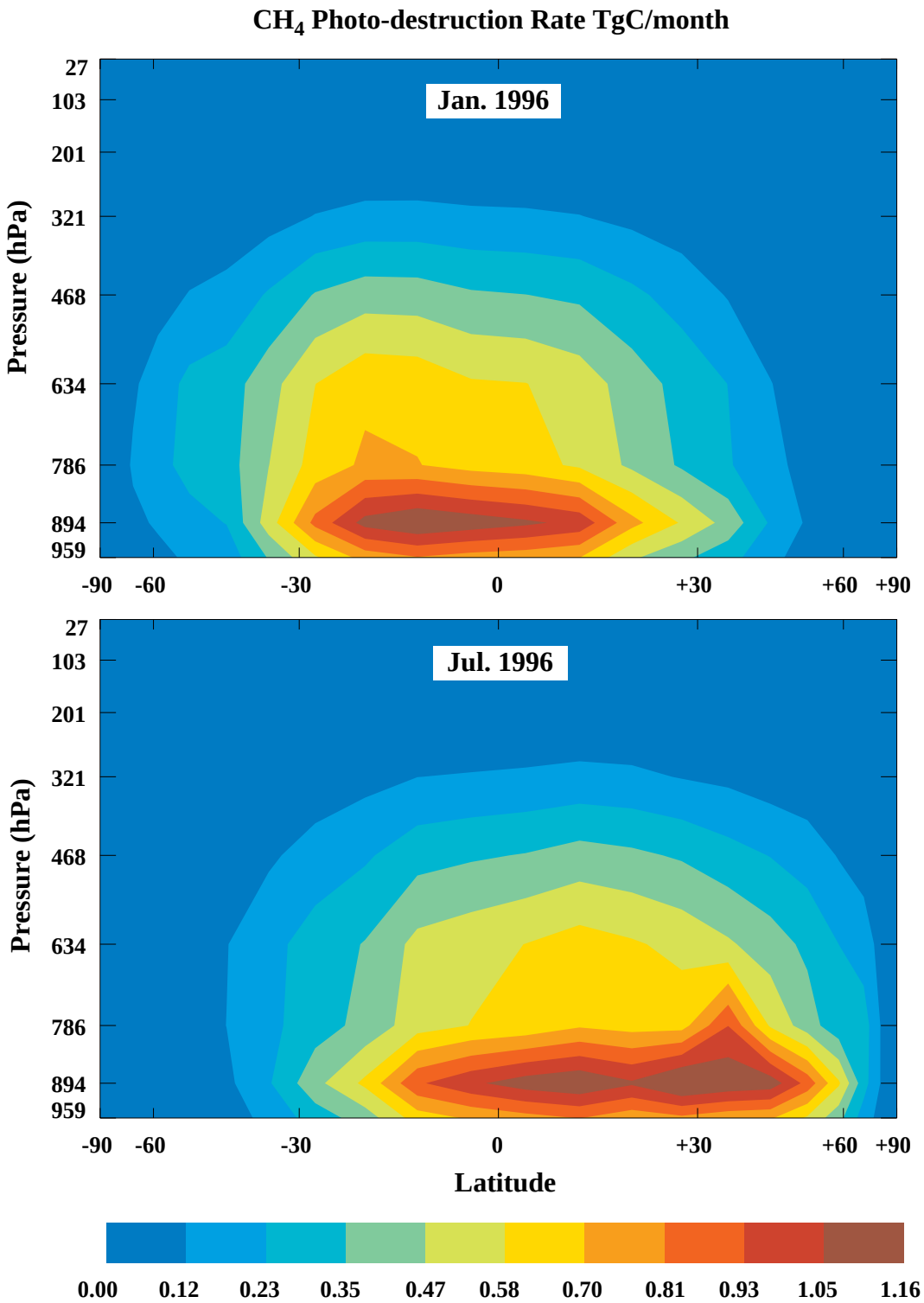

Figure 3. Zonal mean distributions of photochemical destruction rates in TgC per month of methane predicted by the RRR run in January and July 1996, expressed as functions of latitude and pressure level.

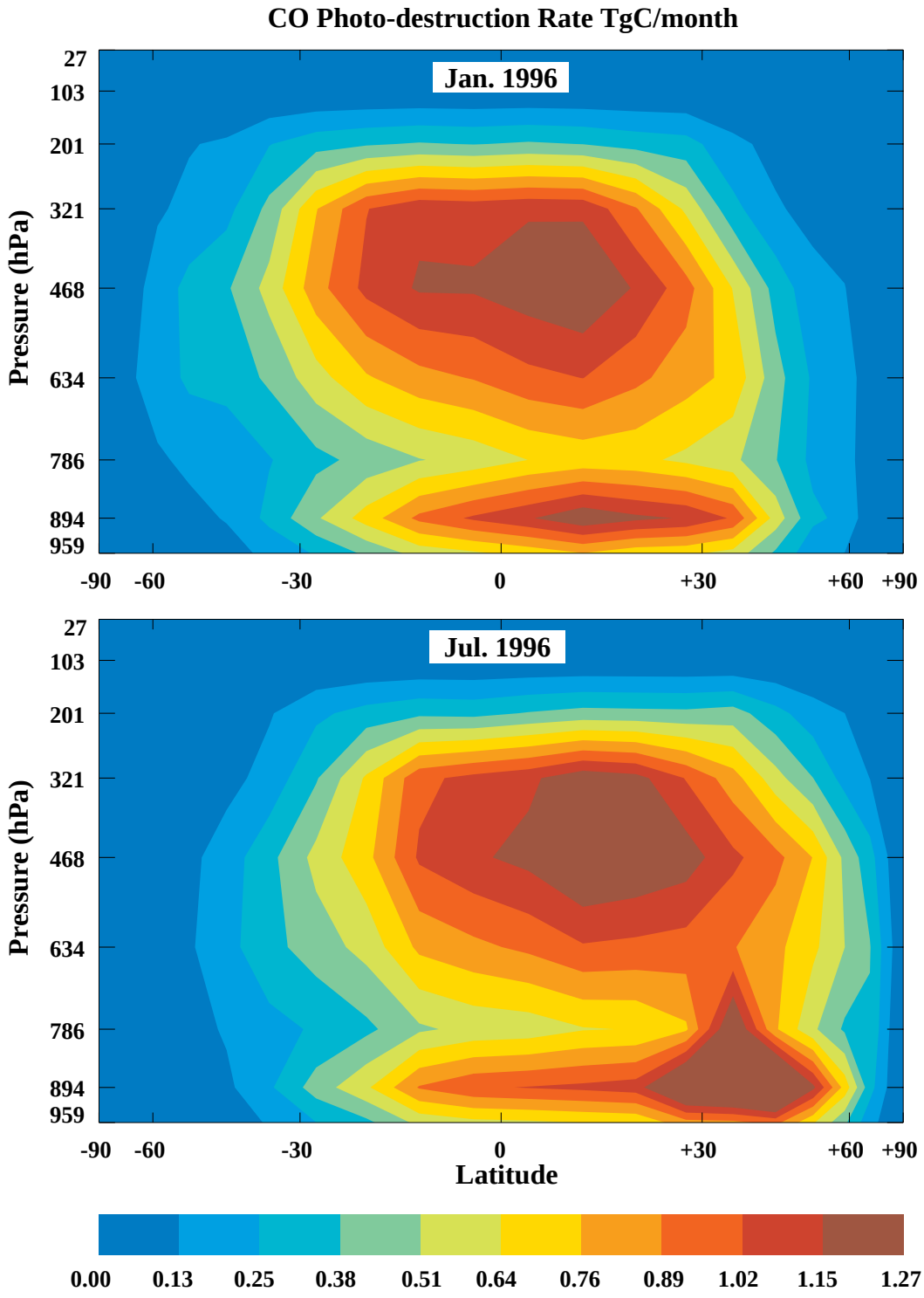

Figure 4. Zonal mean distributions of photochemical destruction rates in TgC per month of carbon monoxide predicted by the RRR run in January and July 1996, expressed as functions of latitude and pressure level.

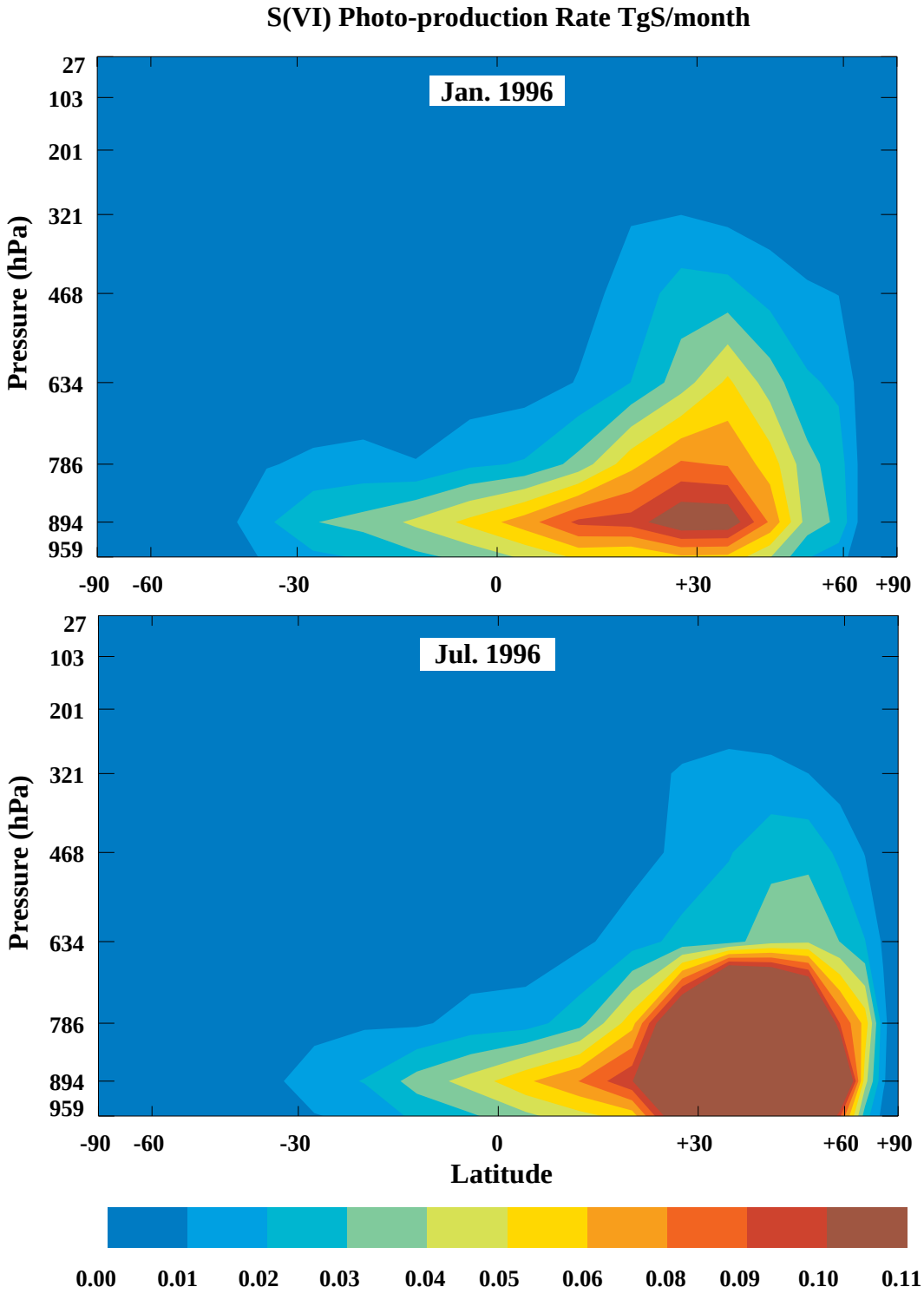

Figure 5. Zonal mean distributions of photo-production rates of sulfate in TgS per month predicted by the RRR run in January and July 1996, expressed as functions of latitude and pressure level.

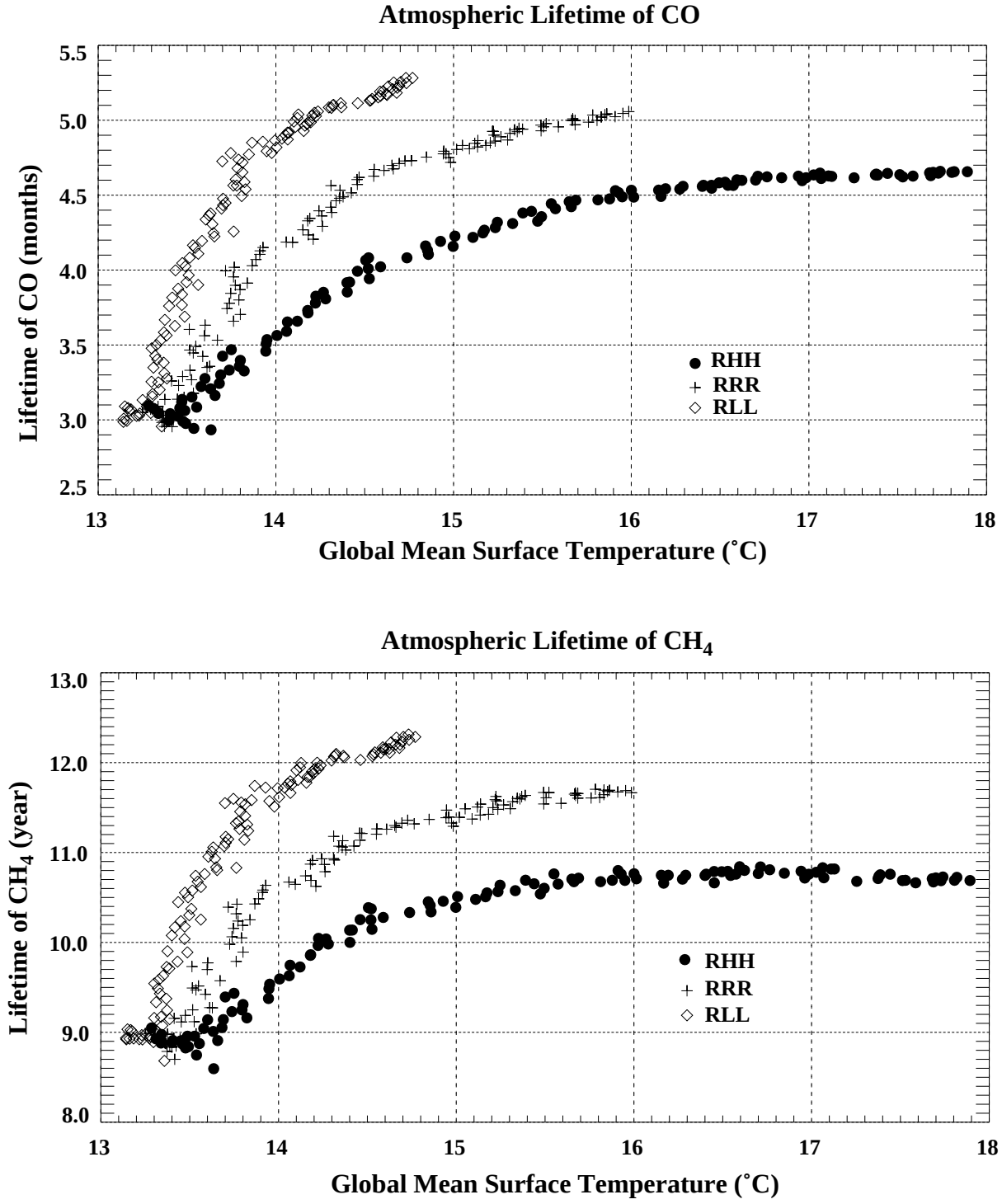

Figure 6. (a) Model predicted, annual-mean atmospheric lifetimes of CO (top panel) and **(b)** CH_4 (lower panel), expressed as functions of annual mean surface temperatures. Each plot contains results from three runs: the RHH (dots), the RRR (crosses), and the RLL (diamonds). *(continued on following page)*

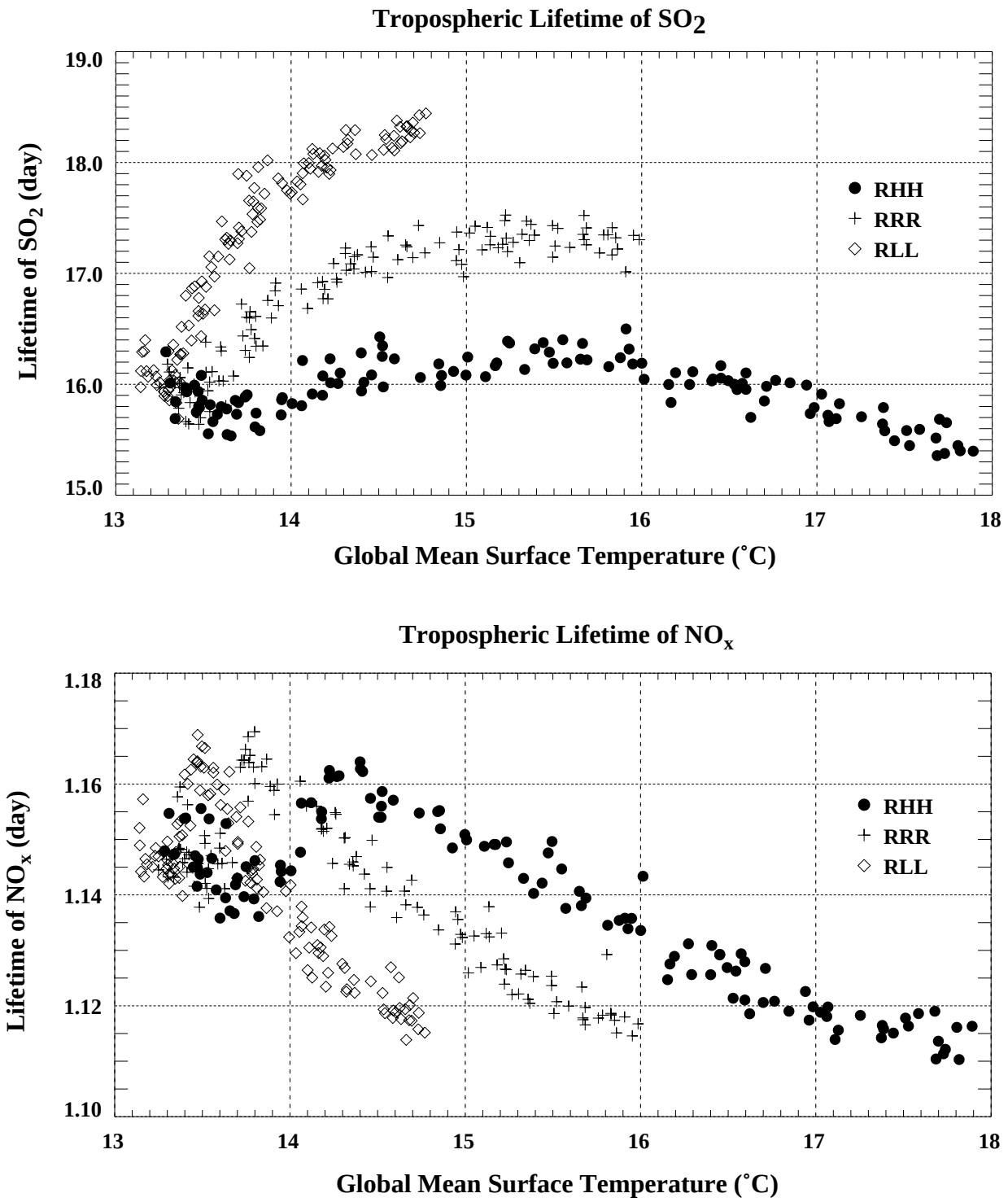

Figure 6 continued. (c) Model predicted, annual-mean tropospheric lifetimes of SO_2 (top panel) and **(d)** NO_x (lower panel), expressed as functions of annual mean surface temperatures. Each plot contains results from three runs: the RHH (dots), the RRR (crosses), and the RLL (diamonds).

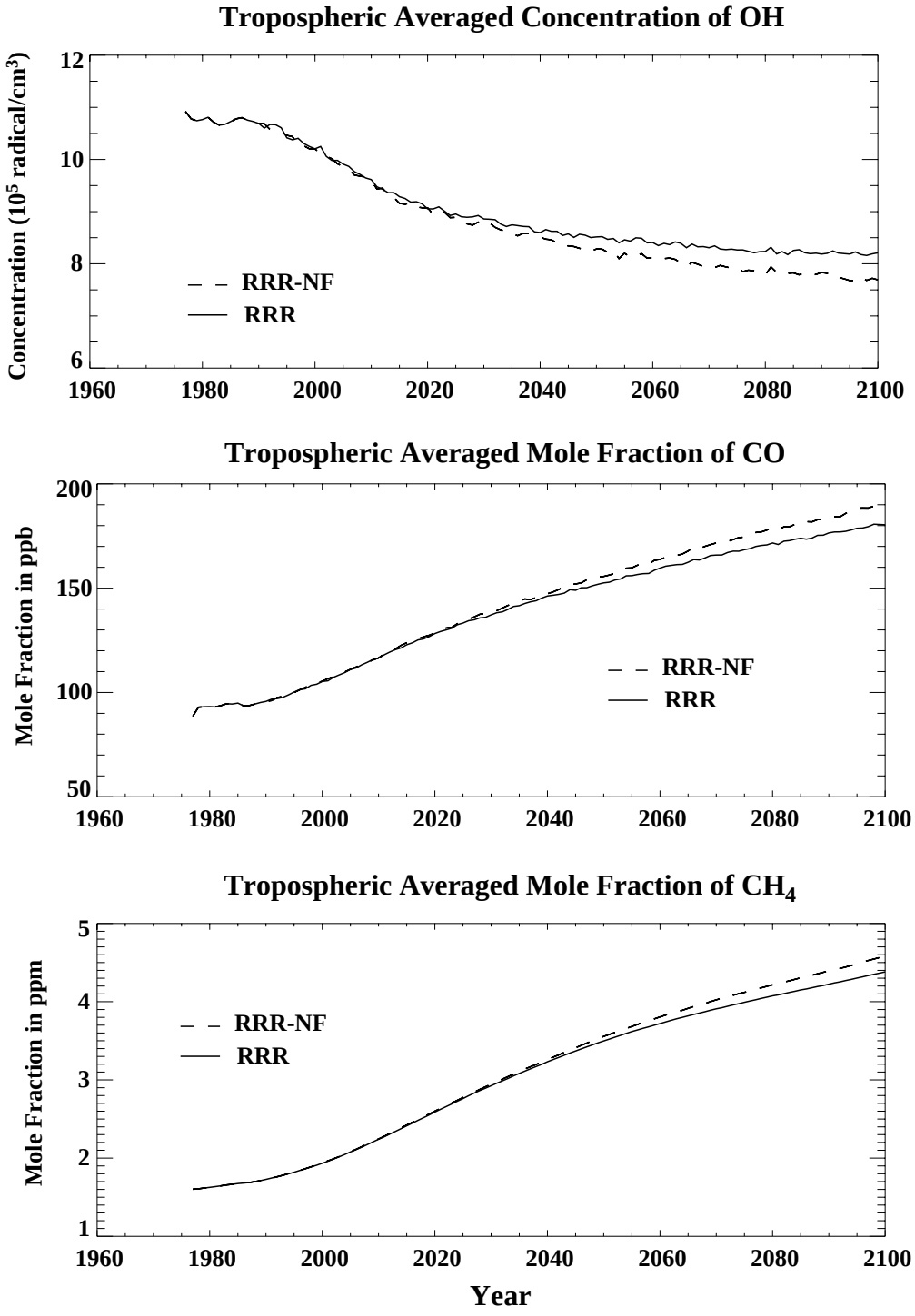

Figure 7. Model predictions of annual-mean tropospheric concentrations of OH (top panel), mole fractions of CO (middle panel), and mole fractions of CH_4 (lower panel). Results derived from the RRR run are plotted as solid lines and those from the RRR-NF run are plotted as dashed lines.

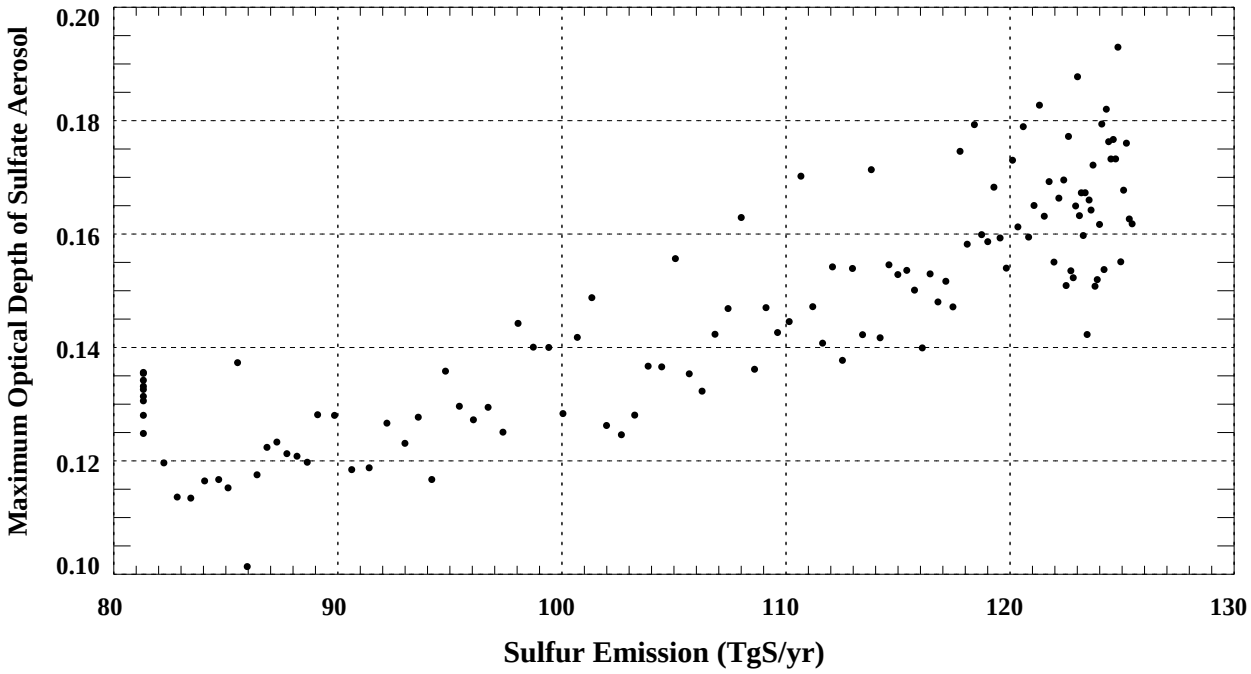

Figure 8. Model predicted correlation between annual sulfur emissions (TgS/yr) and the maximum optical depth of sulfate aerosols above the Earth's surface found in any latitude during the corresponding year. Data are derived from the RRR run.

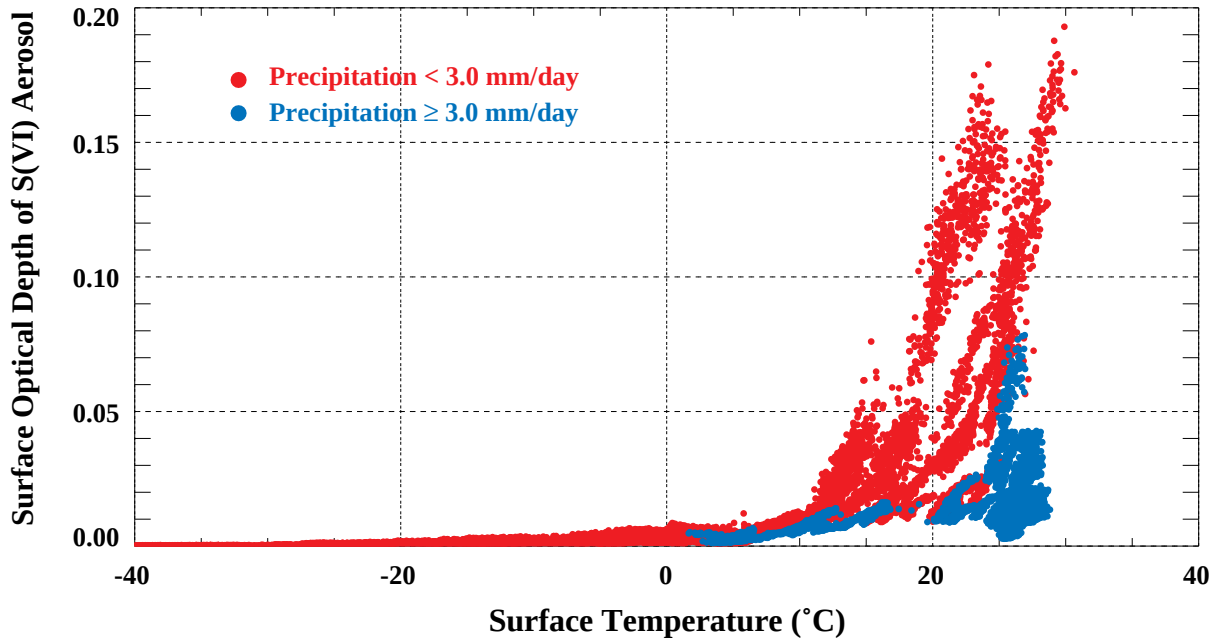

Figure 9. Model predictions of surface optical depths of sulfate aerosols at different latitudes as functions of surface temperature and divided into two groups depending on precipitation rates. Data are from the RRR run.